Fracture Mechanics of Concrete Structures, de Borst et al (eds) © 2001 Swets & Zeitlinger, Lisse, ISBN 90 2651 825 0

Cracking of a saturated hydrated cement system exposed to frost action - numerical modeling

Bruno Zuber
LMT-Département de Génie Civil, Ecole Normale Supérieure de Cachan, Cachan, France
Jacques Marchand
CRIB-Département de Génie Civil, Université Laval, Québec, Canada
Gilles Pijaudier-Cabot
R&DO-Laboratoire de Génie Civil de Nantes - Saint Nazaire, Ecole Centrale de Nantes, France

ABSTRACT: Hydrated cement systems are quasi-brittle porous materials which can be saturated (fully or partially). In service, these materials are often exposed to freezing temperatures. The formation of ice in these systems is known to generate significant internal pressures that may damage the material. Pressures are induced either directly by the formation of an ice crystal or by mass transfers in the weakly permeable medium. In this contribution, a numerical model which predicts the internal micro-cracking of hydrated cement systems subjected to frost action, ice formation and the induced fluid flow motion is presented. Temperature-induced phase transitions of the interstitial fluid are followed using a thermodynamic analysis. The classical Biot's analysis of saturated porous media is used to model the hydro-mechanical behavior of the freezing saturated porous solid and the induced stress state in the solid skeleton. Damage due to microcracking is introduced in the mechanical model. A simple case study aimed at analysing the influence of the relative distance of spherical macropores due to air entrainment is shown as an example of implementation.

1 INTRODUCTION

Hydrated cement systems are quasi-brittle porous materials which can be saturated (fully or partially) with an aqueous solution. In service, these materials may be exposed to freezing temperatures. The formation of ice is known to generate significant internal pressures that may damage the material and induce macrocracks eventually. These pressures are generated either directly by the formation of an ice crystal or by mass transfers in the weakly permeable medium.

It is now quite clear that the freeze-thaw behavior of a porous material exposed to field or laboratory conditions is related to its micro-scale properties and particularly its porosity (Marchand et al. 1995). Laboratory test specimens and field structures differ only in their boundary conditions (physical loading, geometry). However, the physical phenomena involved in both cases are the same. The aim of this study was to elaborate a model that could take into account the various phenomena involved at the 'material' scale in a specimen subjected to frost action (*ice formation*, *mass transfer*, *induced pressures* and *induced damage or cracking*). The final objective of the present research project is to propose a numerical model for quantitative prediction of cracking in concrete structures exposed to any freezing environment.

In our approach, three scales should be distinguished (see Figure (1)) :

- the structural scale (field structure or laboratory test specimen),
- the material scale (mesoscopic scale),
- the pore scale (microscopic or nanoscopic scale).

The pore scale (also called microscopic scale) is used to represent the phenomena occuring into the pores

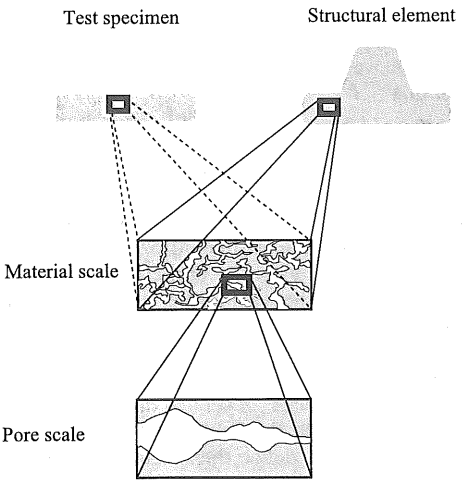

Figure 1: Multiple scale modelling

such as ice formation. On must keep in mind, as it will be seen in Section 3, that pore radii of interest range from a hundred micrometers to only a few nanometers. The material scale, or mesoscopic scale, is introduced to study mass transfers and the mechanical behavior of a representative volume of the material (from the standpoint of frost degradation). The structural scale, or macroscopic scale, should be used to describe the behavior of a structure or a laboratory test specimen (boundary value problems). Although phenomena arising at the structural scale are beyond the scope of this study, some aspects of these problems will be discussed in the last section of this paper.

2 PHYSICAL PHENOMENA

When water freezes, two phenomena occur simultaneously. First, it solidifies (an ice crystal appears) and thus it is able to be mechanically loaded or it may generate pressures. Second, during its solidification, water sees its volume increased by a ratio of 9%. Numerous studies have clearly shown that the frost degradation of cement based materials is mainly related to mass transfer phenomena induced by phase changes occurring in the porous network of the hydrated cement paste. The volume stability of cement systems upon freezing can be better understood by considering the two following cases. On the one hand, ice formation initiated in a fully saturated pore acting as a close and purely elastic container should result in a 9% increase in volume of material. On the other hand, water should be expelled from the pore if the material is permeable and acting as an infinite rigid solid. Reality of course lies between these two cases since the porous medium is deformable and weakly permeable.

Accordingly, water, during the ice formation process, is partially expelled from the freezing sites through the unfrozen pores and towards *external* surfaces. It can be reasonably assumed that the flow of water is laminar in nature. According to Darcy's law, one can relate water pressure gradient to the volumetric water flux :

$$\mathbf{j}_l = -\frac{D}{\eta_l}\mathrm{grad}p_l \qquad (1)$$

D is the permeability of the porous network accessible to the liquid (i.e. of the unfrozen part of the porosity) and η_l is the viscosity of the liquid. During the freezing process, the liquid water either migrates to real external surfaces (i.e. the external boundaries of the material) or to air voids or microcracks. According to Darcy's law, the internal pressures (often called hydraulic pressures) generated during this process will increase with the length of the flow path. This conclusion led to define the spacing factor concept introduced by Powers (see e.g. (Powers 1949)) and yielded the only really efficient practical technique to protect concrete against frost action : the entrainment of a good air bubble network into the cement paste (Marchand et al. 1995). The entrainment of numerous small air bubbles results in a reduction of the mean flow path of water and contributes to significantly decrease the internal pressures induced upon freezing.

As can be seen, the complete description of the volume instability of hydrated cement systems subjected to freezing temperature lies, above all, on a good understanding of the mechanisms of ice formation occuring at the pore scale.

3 POROUS MEDIUM AND ICE FORMATION

In order to model the process of ice formation, one should first describe the salient features of the hydrated cement paste. The medium consists in a solid skeleton, subscript s, and a pore volume. The pore network is geometrically described by its pore size distribution of and its cumulative pore volume $\varphi(r)$:

$$\varphi(r) = \int_r^\infty \frac{\mathrm{d}\varphi}{\mathrm{d}r} dr \qquad (2)$$

where $\varphi(r)$ is expressed in m^3 of pore per m^3 of paste. Its value can be experimentally determined by mercury intrusion porosimetry (Villadsen 1989). The total pore volume represents a fraction (n) of the total volume. n is the porosity defined as:

$$n = \lim_{r \to r_{min}} \int_r^\infty \frac{\mathrm{d}\varphi}{\mathrm{d}r} dr = \varphi(r_{min}) \qquad (3)$$

where r_{min} is the minimum pore radius of the solid (or the minimum pore radius that can be detected by a given experimental technique).

It should be emphasized that ice formation is an incremental process that can be described by the propagation of a curved liquid water/ice interface in the porous network (Zuber et al. 2000). Indeed, as the temperature is decreased, the thermodynamic equilibrium between liquid water and ice is related to the curvature of the interface separating the two phases. Thermodynamic considerations allow to relate the value of the radius of curvature at equilibrium, R_{eq}, to the ambient temperature T. For a material initially saturated with water, these relations indicate that, for a given temperature T, all pores having an entry size radius larger than $Rp_{eq}(T)$ are frozen, while smaller ones remain unfrozen. This process is shown schematically in Figure (2).

A numerical expression for the value of Rp_{eq} as a function of temperature can be found in (Zuber et al. 2000):

$$Rp_{eq} = 0.584 + 0.0052 \cdot \theta - \frac{63.46}{\theta} \quad [\mathrm{nm}] \qquad (4)$$

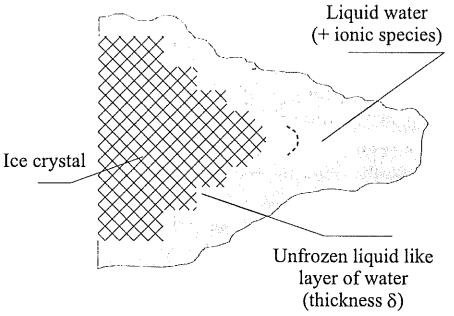

Figure 2: Penetration of a liquid/ice interface in a porous medium - pore scale

This expression is only valid for the freezing phase and another one should be used to describe the behavior of the material upon thawing.

As discussed by Zuber et al. (Zuber et al. 2000), ice formation in a porous solid can then be theoretically predicted on the basis of its pore size distribution. Let us assume that the freezing rate is sufficiently low (i.e. the *rate* of the ice formation is solely controlled by the *rate* of temperature decrease). This corresponds to the situation found in most practical cases where concrete structures are subjected to relatively low freezing rates. The mass of ice formed per unit volume of material during a given temperature interval ($T(t)$ to $T(t+dt)$) can be calculated using the following equation:

$$\frac{1}{V}\frac{\mathrm{d}m_{l\to i}}{\mathrm{d}t} = \rho_i \Phi(t) \tag{5}$$

where ρ_i is ice density, $\Phi(t)$ is the mass increment of ice formation, which is directly related to the pore size distribution and to the radius of curvature at equilibrium for the present temperature, $R_{eq}(t)$. A more detailed study of this phenomenon is proposed in (Zuber and Marchand 2000). It is then possible to predict ice formation in a saturated porous body exposed to freezing and to know which pores are filled with ice and which ones are saturated with liquid water. As a consequence of this continuous process of ice formation, at subzero temperatures, the pore network can be separated in two parts : a frozen part containing ice (subscript i) and an unfrozen part containing liquid water (subscript l).

Additionally, since the system is assumed to be fully saturated (no vapor phase), the relative volume fraction of ice, S_i, and liquid water, S_l, must verify at any time the following relation:

$$S_l + S_i = 1 \tag{6}$$

4 ELASTIC ANALYSIS

4.1 Poro-elastic approach

Like any other porous media, hydrated cement systems are heterogeneous at the microscopic scale. However, at the mesoscopic scale, they can be considered as homogeneous materials. At this scale, the Relative Elementary Volume (REV) is defined as any unit volume at which the porous medium can be considered as homogeneous. Hence one can use theories of porous materials in order to describe the elastic response of the material at the REV level.

Following Biot's theory (Biot 1941), each geometrical point may be considered as a superposition of two continuous media: the porous skeleton and the porosity. It is assumed that both contribute to the stress state of the material. The total stress tensor, $\boldsymbol{\sigma}$, is then the sum of two contributions: that of the solid skeleton called the effective stress tensor, $\boldsymbol{\sigma}$', and a saturated pore volume contribution, $\boldsymbol{\sigma}^*$:

$$\boldsymbol{\sigma} = \boldsymbol{\sigma}' + \boldsymbol{\sigma}^* \tag{7}$$

The pore volume contribution accounts for pressures that may eventually develop in the porosity. Hence $\boldsymbol{\sigma}^*$ can be evaluated by the following equation:

$$\boldsymbol{\sigma}^* = -bp^*\mathbb{I} \tag{8}$$

where $\mathbb{I}$ is the unit tensor and p^* is the mesoscopic pressure which has developed in the pore volume. The parameter b, called the Biot coefficient, is given by:

$$b = 1 - \frac{K}{K_s} \tag{9}$$

where K and K_s are the bulk modulus of the (drained) porous solid and that of the solid skeleton respectively. In this approach, the relation between the effective stress and the elastic strain is given by:

$$\boldsymbol{\sigma}' = \mathbb{C} : \boldsymbol{\epsilon}^e \tag{10}$$

where $\mathbb{C}$ is the elastic tensor of the (drained) porous material (which can be expressed as a function of the elastic modulus (E) and the Poisson coefficient (ν) of the porous solid). The total strain in the porous material, $\boldsymbol{\epsilon}$, is also the sum of several contributions: elastic strains , $\boldsymbol{\epsilon}^e$, and thermal strains $\boldsymbol{\epsilon}^{th}$ (and eventually irreversible strains, $\boldsymbol{\epsilon}^{ir}$):

$$\boldsymbol{\epsilon} = \boldsymbol{\epsilon}^e + \boldsymbol{\epsilon}^{th}(+\boldsymbol{\epsilon}^{ir}) \tag{11}$$

As can be seen from these equations, the prediction of the volume variation of the porous material upon freezing requires the determination of the pressures developed in the pore volume. In the absence of mechanical (external) loads, this pressure growth is equilibrated by the deformable solid skeleton of the material. If the solid skeleton undergoes some variation of stiffness due to damage (microcracking), the internal pressure will change and the mass transfer processes will be modified too.

4.2 Pore pressure

Pressures in ice and in liquid water are assumed to be hydrostatic and equal to p_i and p_l, respectively. As seen in Section 3, ice and water are separated by a curved interface which adopts, at thermodynamic equilibrium, a radius of curvature R_{eq}. It can be shown that the pressures in liquid water and in ice are not equal. A more detailed study of these problems can be found in (Scherer 1999) or in (Zuber and Marchand 2000). According to this approach, the pressure, π_i, exerted on the walls of the pores filled with ice is given by:

$$\pi_i(r,t) = p_l(t) + \chi(r,t) \tag{12}$$

with

$$\chi(r,t) = \gamma_{li}(t) \cdot \left(\frac{2}{R_{eq}(t)} - \frac{1}{r - \delta(t)} \right) \tag{13}$$

As emphasized in Section 4.1, the pressure p^* is already defined as a mesoscopic value. This pressure is the mean pore pressure homogenized over the REV. Knowing that the porosity is partially saturated with water and partially filled with ice, p^* can be evaluated by:

$$p^*(t) = \frac{1}{n} \int_0^\infty p(r,t) \frac{\mathrm{d}\varphi}{\mathrm{d}r}\, dr$$

$$= \overbrace{\frac{1}{n} \int_0^{Rp_{eq}(t)} p_l(t) \frac{\mathrm{d}\varphi}{\mathrm{d}r}\, dr}^{unfrozen\ pore\ contribution} + \overbrace{\frac{1}{n} \int_{Rp_{eq}(t)}^\infty \pi_i(r,t) \frac{\mathrm{d}\varphi}{\mathrm{d}r}\, dr}^{frozen\ pore\ contribution} \tag{14}$$

As described in Section 3, the frozen and unfrozen fractions of the porosity are delineated by the value of Rp_{eq}. On the basis of equations (12) and (13), one can obtain:

$$p^* = p_l + \frac{1}{n} \int_{Rp_{eq}(t)}^\infty \chi(r,t) \frac{\mathrm{d}\varphi}{\mathrm{d}r}\, dr \tag{15}$$

which can be rewritten in a simplified form as:

$$p^*(t) = p_l(t) + X(t) \tag{16}$$

The above considerations assume that ice behaves as a fluid having a finite compressibility but an infinite viscosity (no ice flow).

4.3 Mass transfer

In a multi-component system, the mass conservation of a given phase is studied by following this phase in its own motion. These considerations lead to the development of the general local (from the macroscopic point of view) mass balance equation of a phase k in an open system:

$$\frac{\partial(n_k \rho_k)}{\partial t} + \mathrm{div}(n_k \rho_k \dot{\mathbf{u}}_k) = \mu_{q \to k} \tag{17}$$

with n_k, ρ_k and $\dot{\mathbf{u}}_k$ the volume fraction, the density and the absolute velocity of the phase k respectively. $\mu_{q \to k}$ is a sink/source term, which represents the rate of mass change from phase q to phase k, $\forall\, q \neq k$.

As seen in section 3, our system consists in three phases: the solid skeleton, the liquid water and ice. Their respective volume fractions are given by $(1 - n)$, $n_l = nS_l$ and $n_i = nS_i$. The relative velocity of ice with respect to the solid skeleton is assumed to be equal to zero ($\mathbf{v}_i = 0$ and then $\dot{\mathbf{u}}_i = \dot{\mathbf{u}}$). Liquid water has the ability to flow through the porous network under a pressure gradient as described by equation (1).

Moreover, the rate of mass change from one phase to another is only related, in the present case, to ice formation and $\mu_{q \to k}$ of Equation (17) is reduced to $\mu_{l \to i}$. Using Equation (5), one can directly identify that:

$$\mu_{l \to i} = \rho_i\, \Phi(t) \tag{18}$$

We can now recall the definitions of the coefficient of thermal expansion (isobaric), α_k, and bulk modulus of compressibility (isothermal), K_k of phase k:

$$\alpha_k = \frac{-1}{\rho_k} \left. \frac{\partial \rho_k}{\partial T} \right|_{p_k} \quad \text{and} \quad K_k = \frac{+1}{\rho_k} \left. \frac{\partial \rho_l}{\partial p_k} \right|_T \tag{19}$$

These expressions define the constitutive relations for ice, liquid water and solid skeleton (which is affected either by the pore pressure, p^* and by the effective stress tensor, $\boldsymbol{\sigma}$').

Combining these relations with ice formation introduced through equation (18), the description of the mesoscopic (material scale) behavior of the saturated porous system during freezing relies on the following non-linear system of equations (Zuber and Marchand 2000):

$$\mathrm{div}\boldsymbol{\sigma} = \mathrm{div}\,(\boldsymbol{\sigma}' - bp^*\mathbb{I}) = 0 \tag{20}$$

$$\beta\, \dot{p}_l = \mathrm{div}\left(\frac{D}{\eta_l} \mathrm{grad} p_l \right) - b\, \mathrm{div}\dot{\mathbf{u}} + S \tag{21}$$

with

$$\beta = \frac{nS_l}{K_l} + \frac{nS_i}{K_i} + \frac{b - n}{K_s} \tag{22}$$

$$S = \left(1 - \frac{\rho_i}{\rho_l} \right) \Phi(t) + \bar{\alpha} \dot{T} - \frac{b - n}{K_s} \dot{X} - \frac{nS_i}{K_i} \dot{\kappa} \tag{23}$$

$$\bar{\alpha} = nS_l \alpha_l + nS_i \alpha_i + (b - n)\alpha_s \tag{24}$$

The input data needed to run this model are:

1. the physical properties of the material (porosity and the associated pore distribution, initial per-

meability, coefficient of thermal expansion, bulk modulus);

2. the mechanical and thermal properties of ice (bulk modulus and coefficient of thermal expansion);

3. the physical properties of the interstitial liquid (bulk modulus, coefficient of thermal expansion, viscosity and surface tension);

4. thermo-mechanical loading and boundary conditions (temperature and pressure).

Information on the first three series of data can be found in reference (Zuber and Marchand 2000). Loading and boundary conditions must be adequately chosen to be as relevant as possible to the problem to be solved, and will therefore depend on the situation considered.

5 FREEZE-THAW DETERIORATION

We are going now to introduce the effect of microcracking in the above formulation. For this purpose, we will use the framework of a scalar continuum damage model and see how microcracking due to freezing can be introduced.

Studies on the behavior of concrete at high temperature have shown that damage could be considered as a partition between a purely mechanical damage variable and a purely thermal one (Stabler and Baker 2000). Thermal damage at high temperatures can be directly related to temperature because it is induced by physico-chemical changes in cementitious hydrates. Similarly, we suggest that the damage induced to hydrated cement systems subjected to sub-freezing temperatures can be adequately reduced to two different mechanisms (which implies a dual-damage variable theory). A purely mechanical damage can be generated at the mesoscopic level (for instance by an externally induced state of dilation or expansion). A second damage process can be introduced, directly related to freezing. Then, one of the two following relations could be used for the solid skeleton:

$$d = d_{mechanical} + d_{freezing} \tag{25}$$

or

$$(1-d) = (1-d_{mechanical}) \cdot (1-d_{freezing}) \tag{26}$$

under the condition that the damage variable d ranges between 0 (undamaged) and 1. Two damage variables are introduced in the model because they represent two very different mechanisms. Mechanical damage is due to external loads and produces microcraking. Thermal damage results from the development of internal pressures in the solid skeleton and is characterized by a modification of the pore structure of the material. Evidence of frost-induced pore structure alterations has recently been brought forward. For instance, ice formation and mercury intrusion porosity data reported by Jacobsen (Jacobsen 1995) tend to indicate that frost damage contributes to coarsen the pore structure of hydrated cement systems. Some researchers tried to take into account this phenomenon to describe the behavior of saturated porous materials subjected to freeze-thaw cycles (Salmon et al. 1997). Thermal damage can be considered as the creation of a series of microvoids or the evolution of pore size distribution following the collapse of pore walls due to internal ice pressure at the micro-scale. This degradation process can be modeled using an approach similar to that of (Cowin and Nunziato 1983) or (Pijaudier-Cabot and Burlion 1996) in which porosity serves as a damage variable.

Thermal damage is triggered by ice formation and mass transfer due to the desequilibrium of pressure between ice and liquid water. Pressures generated in the porosity are related to thermal loading (temperature and cooling rate), to fluid flow, and then to $p^* = f_1(T, \dot{T})$. In the present paper, we shall examine two simple test cases. The first one is the situation where damage is imposed as an external variable (for instance if a damage process is due to external mechanical loads). The second situation is the result of a damage process resulting from dilations induced by the flow of water upon freezing. In this case, we consider $d_{freezing}$ as a function of pressure, p^*, generated in the porosity. Equivalently, $d_{freezing}$ is a function of the amount of positive strain induced to the skeleton by this internal pressure:

$$d_{freezing} = 1 - \frac{\tilde{\epsilon}_0(1-A_t)}{\tilde{\epsilon}} - \frac{A_t}{\exp(B_t(\tilde{\epsilon}-\tilde{\epsilon}_0))} \tag{27}$$

where A_t, B_t and $\tilde{\epsilon}_0$ are material characteristics (taken hereafter respectively at 0.8, 10000 and 1.10^{-4}), and $\tilde{\epsilon}$ is the equivalent strain :

$$\tilde{\epsilon} = \sqrt{\sum_{i=1}^{3} \left(\frac{|\epsilon_i| + \epsilon_i}{2} \right)^2} \tag{28}$$

with ϵ_i ($i \in [1,3]$) the principal strains.

In both cases, damage affects elastic properties in a classic way ($\mathbb{C} = (1-d) \cdot \mathbb{C}_0$) (subscript 0 indicates the undamaged properties). In fact, equation (26) is used in oder to introduce damage in the poroelastic formulation. We use a damage model which is similar to the one by Stabler (Stabler and Baker 2000), or Gerard (Gerard et al. 1998). In the model, the permeability of the material does increase with the degree of damage according to the following exponential equation:

$$D = D_0 \exp(16 \cdot d) \tag{29}$$

It should however be emphasized that, in its present state, the model is based on the assumption that the ice formation is not affected in any way by damage. This assumption is clearly an oversimplification of the problem.

6 NUMERICAL ANALYSIS OF A BASIC CASE

If a finite elements approach is chosen to solve this problem, the discretization leads to the following expressions:

$$\mathbb{K}\mathbf{u} - \mathbb{Q}\mathbf{p}^* = \mathbf{f}^u_{ext} \tag{30}$$

$$\mathbb{Q}^T\dot{\mathbf{u}} + \mathbb{H}\mathbf{p}_l + \mathbb{S}\dot{\mathbf{p}}_l = \mathbf{f}^p_{ext} \tag{31}$$

With $\mathbb{K}, \mathbb{S}, \mathbb{Q}$ and $\mathbb{H}$ ad hoc matrices. Nodal unknowns of the problem are the pressure and displacement vectors, respectively $\mathbf{p}_l$ and $\mathbf{u}$. The relation between $\mathbf{p}_l$, the liquid water pressure and $\mathbf{p}^*$, the mesoscopic pressure exerted on pore walls by water and ice is simply introduced through equation (16). This system can be solved numerically either directly (fully coupled) or with a pseudo-coupled scheme (each equation being solved one after the other until convergence is obtained).

In the simple structural case considered in this paper, we look at a material in which air bubbles have been entrained. The basic cell is a spherical shell made of this porous material surrounding an air bubble, as schematically described in Figure 3. In this problem, we want to look at the influence of the bubble spacing, and we need to consider a boundary value problem. In some sense, the scale at which lies the analysis is macroscopic. In that respect, the attempt by Pickett to solve a similar problem using an analytical approach should be mentioned (Pickett 1953). The inner sphere represents an air bubble and the thickness of the cement paste shell can be linked to flow length concept (see (Pickett 1953) or (Snyder 1998)) and be associated, for instance, to a spacing factor. The flow length parameter is introduced to test the ability of the model to describe the influence of the various shell thicknesses on the behavior of the porous system.

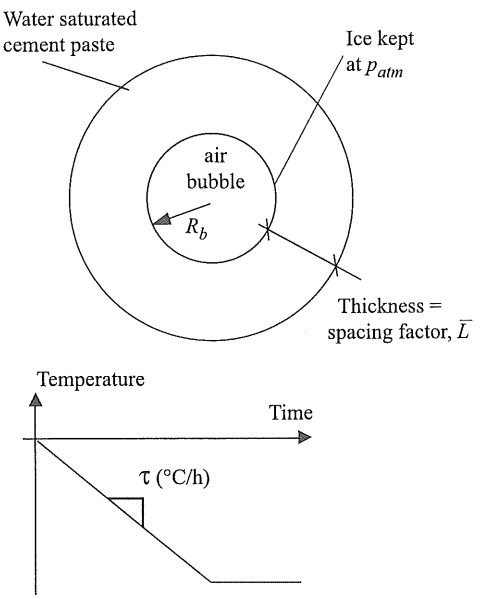

Figure 3: Hollow sphere

The system of equations (30) and (31) is easy to solve in this simplified, spherical, configuration. Equation (31) is reduced to a one dimension equation (variables are only time and radius dependent). The hollow sphere can dilate (or contract) freely and there are no external loads. Verifying equation (30) is equivalent to have $\boldsymbol{\sigma}' = bp^*\mathbb{I}$ (i.e. $\boldsymbol{\sigma} = 0$ in equation (7)).

The system is solely subjected to thermal loading under a linear reduction of the ambient temperature (see Figure 3). The cooling rate is fixed at $-10°C$, approximately the value encountered in laboratory tests, and it is homogeneous over each basic cell.

A constant ice pressure equal to the atmospheric pressure is imposed on the inner sphere. Air bubbles are not water saturated, under freezing conditions ice present in the bubbles and on the inner sphere of the paste shell is at the atmospheric pressure. A zero pressure gradient on the external sphere is imposed. Indeed, the spacing factor value defines the sphere of influence of the air bubble. Then a point A, located on the external sphere of the paste shell also belongs to the sphere of influence of a neighboring air bubble. Since temperature is assumed to be uniform, A is a point of symmetry and the pressure gradient at this point must be zero (which, according Darcy's law, corresponds to a zero flux of water).

All the properties used for the calculations are those of a 0.7 water to cement ratio. The characteristics of the hydrated cement paste can be found in Table 1 of reference (Zuber and Marchand 2000). The preparation of this paste was done under vacuum to avoid any air entrainment thus providing a paste having, the properties of the matrix which would surrounded air bubbles in an air entrained mixture. An important point to note is that permeability is assumed to be reduced as porosity is progressively filled with ice.

The elastic response depicted in Figure 4 clearly shows that the spacing factor is a very important parameter of the problem. A trend of the same kind is observed when the cooling rate is increased or if permeability is decreased (the three contribute to tighten the system and, then to hinder the pressure dissipation).

As discussed in Section 5, damage can be introduced in two ways. The first one is to consider that

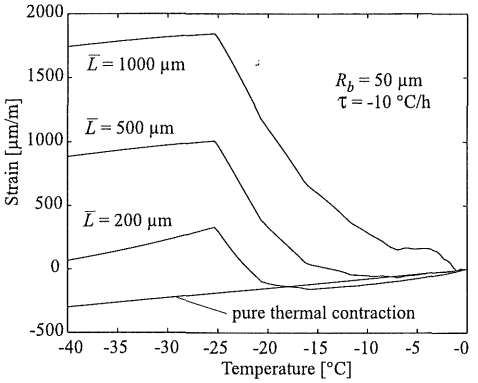

Figure 4: Spacing-factor

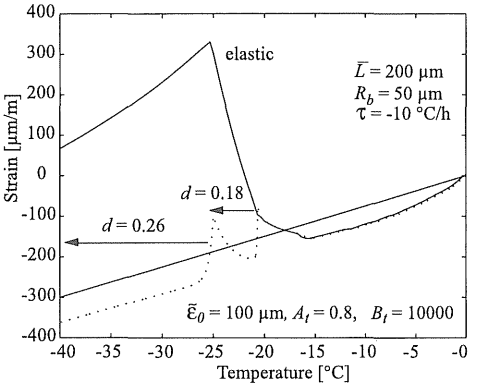

Figure 6: Thermal damage effect during freezing

damage process is imposed to the system studied here (for instance a damage produced in the material by a structural loading at the macroscopic scale). It will be referred to as the external damage case.

In Figure 5 as can be seen damage tends to reduce dilation of the material. This phenomenon is related to the evolution of permeability when the material is damaged.

Let us now consider the second case in which damage is triggered by the extension in the shell due to freezing. In the present calculation, we shall compute damage according to the average value of the strain over the shell thickness. As can be seen in Figure 6, similarly to what had been observed in the previous case (referred to as *external damage case*), damage contributes to reduce the dilation of the material upon

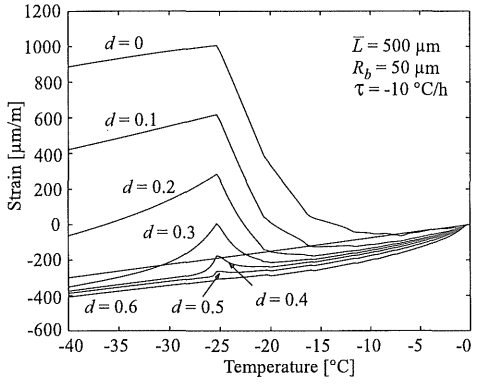

Figure 5: Frost behavior when external damage is imposed

freezing by the deterioration of the material properties.

In addition, we can note that the minimum temperature reached during a test may play an important role. Indeed, when the temperature is decreased, all other parameters being kept constant, damage can be increased as can be observed experimentally.

The above results (for external damage and simplified freezing damage cases) tend to indicate that damage would reduce the dilations induced upon freezing. However this is in contradiction to experimental data which indicate that the dilations tend to increase with damage (see (Jacobsen 1995)). The fact that dilations seem to be reduced by an increase in damage in our calculations is due to the oversimplification made in the analysis. Indeed, permeability and mechanical properties were considered affected by damage (which is a reality) but pore size distribution (and thus ice formation) was not. This apparent contradiction will have to be explained by a specific investigation of the relations between freezing damage and pore size distribution variations. In other words, one could say that the introduction of a freezing damage parameter only linked to mechanical properties is not sufficient and the analysis should be completed with porosity-related considerations (see the simplified attempt in (Salmon et al. 1997), and the mechanical approaches in (Cowin and Nunziato 1983) and (Pijaudier-Cabot and Burlion 1996)). If macro-pores are created (in addition to or in place of micro-pores) during the damage process, more ice would be formed at the same time at rather high (even if sub-freezing) temperatures. Then induced water flow could be increased enough to create additional damage and then explain the experimentally destructive phenomenon observed upon freeze-thaw cycles.

7 CONCLUSION

Based on a multi-scale approach, a numerical model has been devised to simulate damage in cement based materials exposed to frost action. Ice formation mechanisms and physical phenomena generated at the pore scale are taken into account. Two simplified cases

have been investigated in order to see the effect of damage on the frost resistance of the material.

It is clear that transfer properties are major parameters when one tries to model the frost behavior of a cement based material. Evolution of damage and of transfer properties and porosity characteristics with damage is also very important in this process. This work is a first step towards a global modeling of frost action mechanisms. Additional physical phenomena like ice lensing or surface scaling in presence of deicing salts could also be considered in subsequent works.

REFERENCES

Biot, M. A. (1941). General theory of three-dimensional consolidation. *Journal of Applied Physics 12*, 155–164.

Cowin, S. C. and J. W. Nunziato (1983). Linear elastic materials with voids. *Journal of Elasticity 13*, 125–147.

Gerard, B., G. Pijaudier-Cabot, and C. La Borderie (1998). Coupled diffusion damage modelling and the implications on failure due to strain-softening. *International Journal of Solids and Structures 35*, 4107–4120.

Jacobsen, S. (1995). *Scaling and cracking in unsealed freeze/thaw testing of Portland cement and silica fume concretes.* Ph. D. thesis, University of Trondheim, Department of Civil Engineering, Trondheim, Norway. 286 p.

Marchand, J., R. Pleau, and R. Gagné (1995). Deterioration of concrete due to freezing and thawing. In *Material Science of Concrete*, Volume IV, pp. 283–354. Westerville, OH, USA: American Ceramic Society.

Pickett, G. (1953). Flow of moisture in hardened portland cement paste during freezing. In *Proceedings of the Highway Research Board, Bulletin 46*, Volume 32, pp. 276–284.

Pijaudier-Cabot, G. and N. Burlion (1996). Damage and localisation in elastic materials with voids. *Mechanics of Cohesive-Frictional Materials 1*, 129–144.

Powers, T. C. (1949). The air requirement of frost-resistant concrete. In *Proceedings of the Highway Research Board, PCA Bulletin 33*, Volume 29, pp. 184–211.

Salmon, E., M. Ausloos, and N. Vandewalle (1997). Aging of porous media following fluid invasion, freezing and thawing. *Physical Review, The American Physical Society 55*(6), 1–4.

Scherer, G. W. (1999). Crystallization in pores. *Cement and Concrete Research 29*(8), 1347–1358.

Snyder, K. A. (1998). A numerical test of air void spacing equations. *Advanced Cement Based Matererials 8*, 28–44.

Stabler, J. and G. Baker (2000). On the form of free energy and specific heat in coupled thermo-elasticity with isotropic damage. *International Journal of Solids and Structures 37*, 4691–4713.

Villadsen, J. (1989). The influence of curing temperature on pore structure of hardened cement paste. Technical Report 218/90, Lab. for Bygn. Mat., Danmarks Tekn. Højskole.

Zuber, B. and J. Marchand (2000). Modeling the deterioration of hydrated cement systems exposed to frost action - part 1: Description of the mathematical model. *Cement and Concrete Research 20*(12), 1929–1940.

Zuber, B., J. Marchand, A. Delagrave, and J.-P. Bournazel (2000). Ice formation mechanisms in normal and high-performance concrete mixture. *Journal of Materials in Civil Engineering, ASCE 12*(1), 16–23.